Journal of Organometallic Chemistry 695 (2010) 2191–2200

Contents lists available at ScienceDirect

Journal of Organometallic Chemistry

journal homepage: www.elsevier.com/locate/jorganchem

Palladacycles with *C,N*-bidentate and *N,C,N′*-tridentate ligands: Structures, spectral study and catalytic methanolysis of P═S pesticides

Zhong-Lin Lu [a,*], Xue-Rui Wang [a], Bian-Bian Liu [a], Rui-Yao Wang [b]

[a] The College of Chemistry, Beijing Normal University, Xinjiekouwai Street 19, Beijing 100875, China
[b] Department of Chemistry, Queen's University, Kingston, Ontario, Canada K7L 3N6

ARTICLE INFO

Article history:
Received 25 February 2010
Received in revised form
28 May 2010
Accepted 3 June 2010
Available online 15 June 2010

Keywords:
Palladacycle
Crystal structure
Methanolysis
Pesticides
Kinetics

ABSTRACT

Palladacycles **2**–**4** with *C,N*-bidentate and *N,C,N′*-tridentate ligands were prepared and characterized. The X-ray crystal structures of [2,6-bis(*N,N*-dimethylaminomethyl)phenyl-N,C^1,N′-](aqua)palladium(II) triflate (**2**), (*N,N*-dimethylaminobenzyl-C^1,N)(4-trifluoromethylpyridine)(aqua)palladium(II) triflate (**3**), and (*N,N*-dimethylaminobenzyl-C^1,N)(4-*N,N*-dimethylaminopyridine)(aqua)palladium(II) triflate (**4**), were determined. While **2** is much less active, **3** and **4** effectively catalyze the methanolysis of the P═S pesticides. The catalytic activities were higher with the trifluoromethylpyridine co-ligand as compared to palladacycles containing 4-*N,N*-dimethylaminopyridine and pyridine co-ligands. ^{1}H NMR spectra and the catalytic kinetic dependences on concentration and pH revealed that the active species was a palladacycle containing one methoxide and one pyridine in the coordination sphere. A plot of the catalytic activity vs. free [pyridine] indicated the participation of a common species. The proposed catalytic mechanism involves a pre-equilibrium binding of the P═S pesticide to palladium(II) center followed by dissociation of the pyridine and subsequent cleavage of the P–OAr unit through the intramolecular displacement on phosphorus by the adjacent Pd-coordinated methoxide.

1. Introduction

Phosphorothionate esters are widely used as agricultural pesticides because of their high insecticidal and acaricidal properties and much lower mammalian toxicity than the analogous P═O counterparts [1]. Some chemically related neutral P═O containing organophosphates (OP) are also used as neurotoxins and chemical warfare (CW) agents [2]. Due to their toxicity, lingering effects on the environment, dangers emerging from aging stockpiles and the requirements of the 1992 Chemical Weapons Convention Treaty [3] that signatory nations destroy scheduled CW agents by 2012, the development of efficient methods for the controlled decomposition of these OP materials is of on-going interest.

Many efforts have been directed to the catalytic or enzymatic hydrolysis and oxidation of these organophosphates, but their efficiency and safety still need to be improved [4]. Recently, alternative methodologies, i.e. metal-ion catalyzed alcoholysis, for the rapid decomposition of neutral OP compounds including phosphate triesters, phosphonates, phosphorothionates and phosphonothionates were presented [5]. The advantages of a catalytic alcoholysis method over hydrolysis include greater substrate solubility in the alcohol medium, greatly increased reaction rates probably attributable to a less polar medium that also gives enhanced M^{x+}:substrate pre-equilibrium complexation [5g], and the fact that the products are also neutral OP compounds that are non-inhibitory since they bind to the metal catalyst with a similar strength as the starting OP materials. Lanthanides such as La^{3+}, being "hard" metal ions in the Pearson "hard/soft" sense, can accelerate the methanolysis of P═O esters like paraoxon (*O,O*-diethyl *O*-*p*-nitrophenyl phosphate) by $\sim 10^9$-fold [5f], and a 1,5,9-triazacyclononane complex of Cu(II), a "soft" metal ion, was shown to be very efficient for promoting the decomposition of P═S esters like fenitrothion for which La^{3+} is ineffective [5c,h].

It is reported that cyclometalated palladium and platinum complexes effectively catalyze the hydrolysis of phosphorothionates [4d,6]. Our studies [5a] have shown that a palladacycle with coordinated [(*N,N*-dimethylamino)methyl]phenyl, and pyridine ligands, namely Pd(dmba)(py)(OTf), **1**, also promotes the methanolysis of phosphorothionates and shows greater catalytic efficacy and specificity for these P═S derivatives than do any of the Cu(II) complexes that have been investigated [5a]. At higher $^{s}_{s}$pH, the coordinated pyridine in **1** partly dissociated from the Pd and,

* Corresponding author. Fax: +86 10 58801804.
E-mail address: luzl@bnu.edu.cn (Z.-L. Lu).

0022-328X/$ – see front matter © 2010 Elsevier B.V. All rights reserved.
doi:10.1016/j.jorganchem.2010.06.002

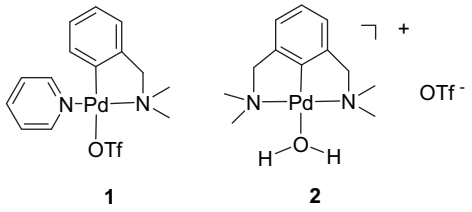

Scheme 1.

according to the $^{s}_{s}$pH/rate profile data, the catalytically active species has a bound methoxide generated with an apparent $^{s}_{s}$pK_a of 10.8. However, whether the catalytically active complex contains a coordinated pyridine or another ligand such as a methanol in addition to the essential coordinated methoxide, was not made clear in that study. Furthermore, the effect of the basicity of the co-ligand pyridine and the reactivity of the widely used pincer palladacycles on the methanolysis needs to be evaluated.

Under the above consideration and with the aim to develop more efficient catalysts, we have prepared some new palladacycles; one with the NCN pincer ligand (**2** in Scheme 1) which provides some additional rigidity to the metal carbon bond by virtue of the two chelating arms and two variants of **1** where pyridine is replaced by two other substituted pyridine ligands (**3** and **4** in Scheme 2) in order to probe the effect of pyridine basicity on the kinetic reactivity. We report here the syntheses, structural characterizations and the kinetic studies of their catalytic methanolysis of fenitrothion (**5**) and turnover experiments for the **3**-promoted methanolysis of some other P═S esters shown in Scheme 3.

2. Results and discussion

2.1. Syntheses of the complexes 2–4

Syntheses of the above palladacycles were straightforward from their corresponding chlorides (see experiment part), the exchange of the counter ion from chloride to triflate with silver triflate with 2 h at room temperature gave good yields of the desired compounds, the structures of which were confirmed by ^{1}H NMR, mass spectra, elemental analysis, and X-ray single crystal characterization. The water molecules that are coordinated to the Pd in the crystal structures in Figs. 1–3 most likely arise from adventitious water in the solvents during preparation and purification. We note that such water molecules often appear in the crystals of many palladacycles containing triflate, despite the crystals being grown from dry solvent. This may suggest energetically favorable interactions with the closely packed triflate counterions in the solid forms. In methanol, where the triflate ions are dissociated from the complex and the [MeOH] greatly exceeds that of adventitious water, there is no reason to expect that water will preferentially bind to the metal ion, which is consistent with the observations that the products of the reaction are derived from methanolysis and not hydrolysis.

2.2. Description of crystal structures of complexes 2–4

The palladium in complex **2** (Fig. 1) is bound to two mutually *trans* NMe_2 moieties, the phenyl carbon (via C(1)) and the oxygen atoms from a water molecule. The geometry around the metal center is a slightly distorted square-planar coordination sphere with C(1)–Pd–O(1) and N(1)–Pd–N(2) angles being 177.04(8)° and 163.73(7)°, respectively. The five-membered metallacycles are puckered in the same direction, with Pd–N1–C7–C2 and Pd–N2–C10–C6 torsion angles of −32.72° and −61.72°, respectively. The bond lengths and angles (see Table 1) are in good agreement with those in $[Pd(NCN)(OH_2)]BF_4$ [7].

For complexes **3** and **4**, the palladium atom displays the expected nearly square planar coordination with the two coordinated nitrogen atoms positioned *trans* to one another. For complex **4**, there are two kinds of molecules in the unit cell with slight differences in bond distances and bond angles. The dihedral angles between the pyridine ring and palladacycle ring are 68.9 and 60.66/61.57° in complexes **3** and **4**, respectively. The dihedral angle between the planes {C1PdN1} and {N2PdO1} in complex **3** is 0.98°, while that in the two molecules of complex **4** equals to 2.19° and 2.45°, respectively, indicating that the square planar coordination geometry is more distorted in **4** than in **3**.

The Pd–C, Pd–N, and Pd–O bond lengths in complexes **3** and **4** (see Table 1) fall within the range of the values reported for other cyclopalladated derivatives of (*N*,*N*-dimethylamino)methylbenzene [5a]. The longer Pd–O (water) bond length of 2.17 Å is attributed to the *trans* effect from the strong σ-donor of the phenyl carbon atom. Surprisingly, the Pd–N (pyridines) bond lengths in complexes **3** and **4** are in good agreement with that in complex **1** (2.035(2) Å), and not effected by the *para* substituent groups on the pyridine ring, no matter whether it is an electron-dononating substituent (*N*,*N*-dimethylamino) or electron-withdrawing substituent (trifluoromethyl). The Pd–C and Pd–N (amine) bond lengths are also not affected.

It can clearly be seen that the Pd–C bonds in complexes **3** (1.967(3) Å) and **4** (1.965(3)/1.973(3) Å) are somewhat longer than that in complex **2** (1.906(2) Å), while the Pd–N (amine) bonds in **3** (2.071(3) Å) and **4** (2.072(2)/2.066(2) Å) are shorter than that in **2** (2.1003(18) Å), which can be attributed to the NCN pincer chelate effect and *trans* effect (pyridine versus amine groups).

In the crystals of compounds **2**, **3** and **4**, each triflate anion is hydrogen-bonded to two water molecules in the coordination sphere, and each water molecule to two triflate anions (see Fig. 4). Palladacycles **2** and **3** are dimerized through H-bonding, while the arrangement in **4** actually gives a contiguous chain. Such intermolecular hydrogen-bonding exists in the crystal lattice of each complex, and plays an important role in stabilizing the ionic structure [7].

2.3. Solution NMR studies of palladacycles 1, 3 and 4 (5×10^{-3} M) in methanol

To obtain information about the speciation of palladacycles in methanol solution as a function of pH, the ^{1}H NMR spectra of **1**, **3** and **4** were studied under different conditions. Since the phenyl-H[6] of the palladacycles, as well as the benzylic CH_2 and NCH_3 protons, are sensitive to changes in the Pd-coordination sphere, their chemical shifts and integrals were studied in more detail.

In methanol-d_4, the ^{1}H NMR spectra of **1**, **3**, and **4** (5×10^{-3} M) are consistent with a single observable material that we assign as palladacycle **11** (see Scheme 4 and Supporting material Figs. S1–S3)

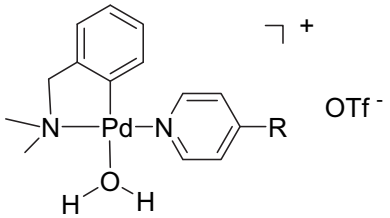

Scheme 2.

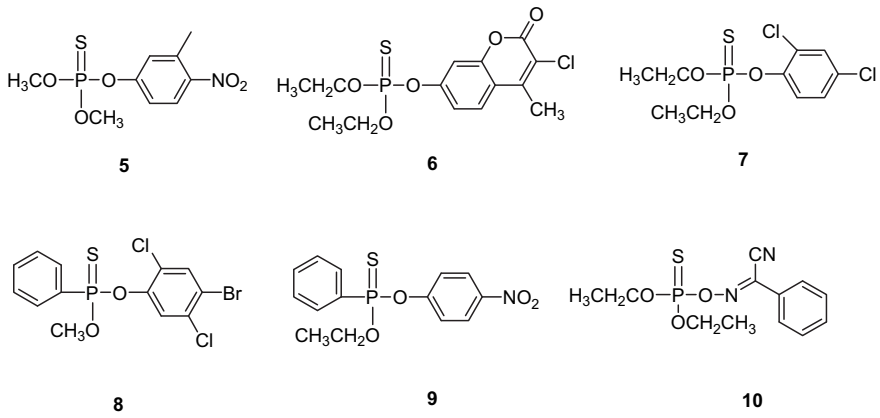

Scheme 3. The phosphorothionate and phosphonothionate pesticides investigated.

due to the typical features of the *N,N-trans*-arrangement [8]. The ratio for the CH_2 and NMe_2 protons is 2:6 as expected and the relative ratios of the phenyl-H^6 signal around 6.0 ppm and pyridine-$H^{2'}$ and -$H^{3'}$ protons are 1:2:2. Upon addition of one equivalent of sodium methoxide to the above solutions, the spectra change visibly. In general the observations with the added methoxide are: 1) broader peaks appearing for new signals arising from pyridine not strongly associated with the Pd; 2) the integrated intensity of H^6 (characteristically upfield of the other phenyl protons due to the presence of the *cis* pyridine on Pd) was decreased as expected if some of the pyridine dissociated; and 3) there were at least two peaks for the CH_2 group as well as for NMe_2. These changes can be attributed to the formation of the methoxy containing palladacycle **12**, and the pyridine dissociated species **13** under strong basic conditions. The ratio of the pyridine coordinated species **12** to ones without a coordinated pyridine can be estimated from the integration ratio of H^6 at *ca.* 6.0 ppm to the total phenyl protons as well as from the integrated ratio of the CH_2 peak from **12** to those of the total CH_2 protons. It was found that the pyridine coordinated species for palladacycle **3**, **1**, and **4** are *ca.* 55%, 66%, and 72%, respectively. Thus, the strong coordinating ligand, *N,N*-dimethylaminopyridine, is slightly less dissociated from the palladacycle, and the more weakly coordinating trifluoromethylpyridine is somewhat more dissociated from the palladacycle in the presence of one eq. of methoxide. The assignment of the NMR peaks for different species observed for palladacycles **1**, **3** and **4** are listed in Table 2. The species **13** from each of the three palladacycles should be the same and exhibit the same chemical shifts. Shown in Supporting information, Figs. S1–S3, include the ^{1}H NMR spectra of the palladacycles in the presence of one equivalent of added methoxide and with dilution from 5 mM to 1.25 mM. Based on the integrated intensities for the CH_2 unit in the presumed methoxy/pyridine forms **12** at ~δ 4.0–4.1 ppm and the species **13** δ 3.83 ppm, it is apparent that dilution does not change the ratio of **12**/**13**, which indicates that **13** is still a monomer. Methoxide species **13** could result in the formation of dimer **14** in the basic solution. However, the dimer **14** is almost absent under the measured condition because the absence of the signal of **14** in the above spectra (see the following experiment).

The signals of **13** and **14** could be inferred from the spectra of the chloro-bridged dimer complex in the presence of base (see Figs. S4a–c). The CH_2 of the chloro-bridged dimer appears at δ 4.01 ppm,

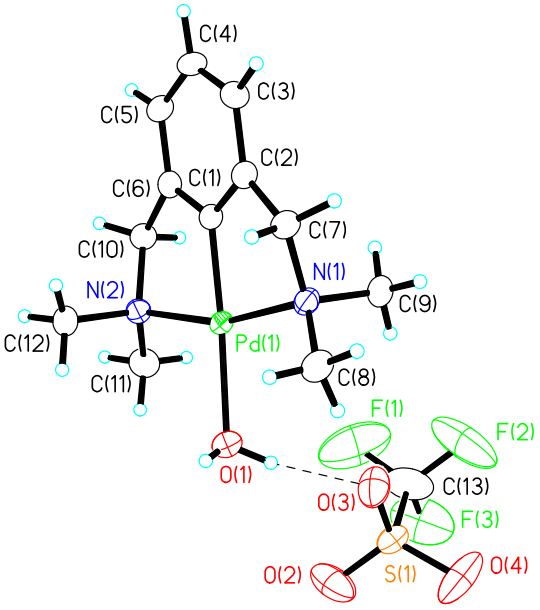

Fig. 1. ORTEP presentation of the molecular structure of **2**. Displacement ellipsoids for non-H atoms are shown at the 50% probability level and H atoms are represented by circles of arbitrary size.

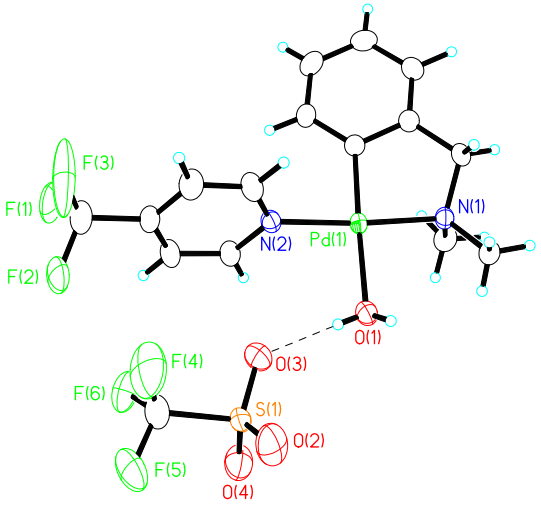

Fig. 2. ORTEP presentation of the molecular structure of **3**. Displacement ellipsoids for non-H atoms are shown at the 50% probability level and H atoms are represented by circles of arbitrary size.

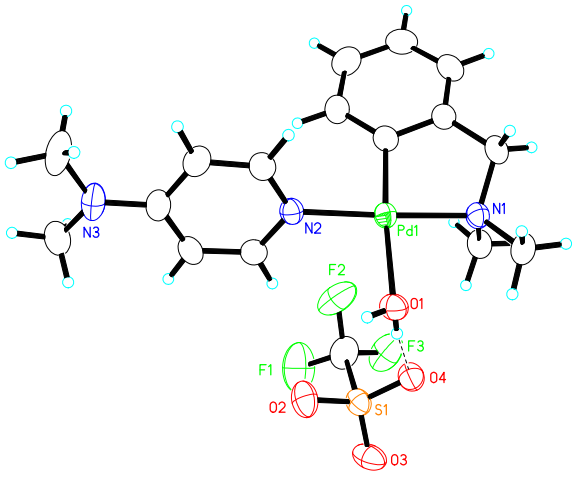

Fig. 3. ORTEP presentation of the molecular structure of **4**. Displacement ellipsoids for non-H atoms are shown at the 50% probability level and H atoms are represented by circles of arbitrary size.

and upon the addition of 1 equivalent NaOMe a new peak at δ 3.83 ppm appeared, which could be assigned to **13**. When 1 more equivalent of NaOMe was added, it was found that the ratio of the peak areas between δ 4.01 ppm and δ 3.83 ppm changed from 1.0:2.9 to 1.5:2.6. The increase of the peak at δ 4.01 ppm can tentatively be attributed to the formation of dimer **14**, which can be assumed to have nearly the same CH_2 chemical shift as dichloro-bridged one.

As a short summary, the pyridine co-ligands in palladacycle **1**, **3**, and **4** are mainly coordinated to palladium under basic conditions, although a small part could be dissociated. Bearing in mind that the kinetic experiments to be discussed employed concentrations of palladacycles that were ~100 times less than those in the NMR studies and the palladacycle was always added at last to the reaction mixture, the catalytic species should be **12** under the kinetic conditions.

2.4. Methanolysis of **5** catalyzed by palladacycles **2**–**4** at low concentrations

In preliminary experiments to determine the activities of **2**–**4** for the methanolysis of fenitrothion **5** in buffered solution, we found that the pincer complex **2** is far less active than compound **3**. In methanol containing triethylamine (TEA) buffered at $^{s}_{s}$pH 10.80, $[\mathbf{5}] = 2.84 \times 10^{-5}$ M and $[\mathbf{3}] = 2 \times 10^{-5}$ M, $k_{obs} = 6.46\ min^{-1}$, while that for the **2**-catalyzed process under the same conditions is

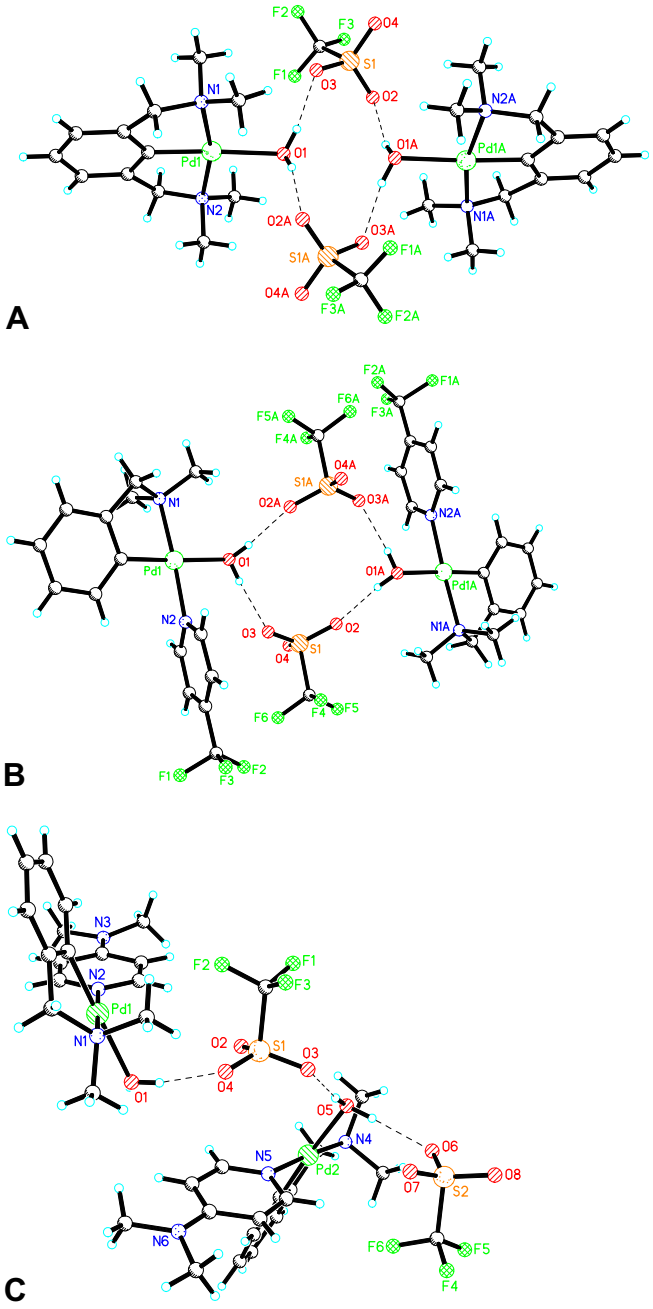

Fig. 4. Hydrogen-bonding networks in the complexes **2** (A), **3** (B), and **4** (C).

Table 1
Selected bond lengths [Å], bond angles [°] and torsion angles [°] for **2**, **3**, and **4**.

Parameter	2	3	4
Pd(1)–C(1)	1.906(2)	1.967(3)	1.965(3)/1.973(3)
Pd(1)–O(1)	2.1838(18)	2.169(3)	2.174(2)/2.178(2)
Pd(1)–N(1)	2.1003(18)	2.071(3)	2.072(2)/2.066(2)
Pd(1)–N(2)	2.1025(19)	2.042(3)	2.038(2)/2.041(2)
C(1)–Pd(1)–N(1)	81.87(8)	82.56(12)	82.35(10)/82.44(10)
C(1)–Pd(1)–N(2)	81.88(8)	93.05(12)	94.18(10)/93.86(10)
N(1)–Pd(1)–N(2)	163.73(7)	175.51(10)	176.18(9)/175.91(9)
C(1)–Pd(1)–O(1)	177.04(8)	177.86(11)	174.51(11)/174.63(10)
N(2)–Pd(1)–O(1)	96.03(7)	89.09(10)	91.10(9)/91.22(9)
N(1)–Pd(1)–O(1)	100.19(7)	95.31(11)	92.32(9)/92.43(9)
C(1)–Pd(1)–N(1)–C(9)	−91.85(16)	−87.8(2)	151.07(19)/150.4(2)
N(2)–Pd(1)–N(1)–C(9)	−94.3(3)	−99.7(13)	176.0(12)/175.8(12)
O(1)–Pd(1)–N(1)–C(9)	90.31(16)	92.2(2)	−30.26(18)/−31.15(19)

$0.0015\ min^{-1}$, i.e. about 4300 times slower. Thus, further kinetic work focused on compounds **3** and **4**.

Following procedures previously described for **1** [5a], the kinetics for methanolysis of **5** were determined as a function of [**3**] and [**4**] at $^{s}_{s}$pH 10.80 (TEA buffer, extrapolated to [TEA] = zero) and the k^{obs}_{max} values vs. [**3**] and [**4**] data (given in Table S1 of the supporting material) are plotted in Fig. 5. The plots are linear with no curvature, indicative of a kinetically active monomeric form of **3** and **4** without evidence of any appreciable amount of kinetically active or inactive dimer in equilibrium with the monomeric forms at these low concentrations. If dimers were kinetically important or prevalent, but non-active, one would expect the plots to curve upward and downward, respectively. The second order rate constants for the catalytic processes (k^{obs}_{2}), evaluated as the

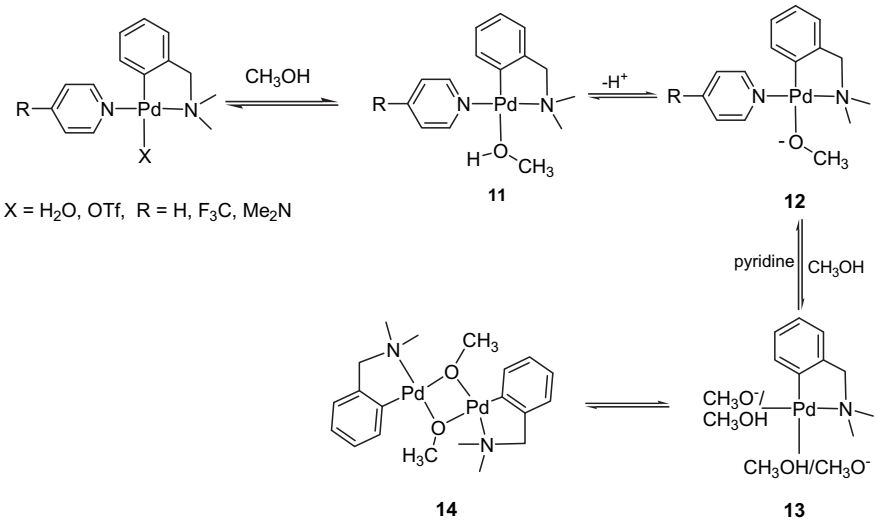

Scheme 4. The possible speciation of palladacycles in methanol and basic methanol solutions.

gradients of the linear plots, are listed in Table 3. These indicate that the activities of **1**, **3** and **4** are inversely dependent on the basicity of their corresponding pyridines, the ordering of reactivity being **3** > **1** > **4** in a ratio of 38:13:1.

The pseudo-first order rate constants (k_{max}^{obs}) determined after extrapolation to [buffer] = 0 for the methanolysis of **5** promoted by 2.0×10^{-5} M solutions of **3** and **4** at ${}^{s}_{s}$pH values between 8.22 and 12.23 are presented in Table S2 (Supporting Information). The corresponding k_2^{obs} values for complexes **1**, **3** and **4**, obtained as $k_{max}^{obs}/(2 \times 10^{-5}$ M), are plotted in Fig. 6. The appearance of the plots suggests a process where the basic form of the catalyst is active as in eq. (1) for which can be derived the kinetic expression given in eq. (2). NLLSQ fittings of the data give the k_2^{max} and kinetic ${}^{s}_{s}pK_a$ values listed in Table 2 and best fit lines through the data are shown in Fig. 6.

$$^{-}OTf + L : Pd(II) : HOCH_3 \underset{K_a}{\overset{-H^+}{\rightleftharpoons}} L : Pd(II) : {}^{-}OCH_3 \xrightarrow[k_2^{max}]{5} P \qquad (1)$$

$$k_2^{obs} = k_2^{max}\left(10^{-pK_a}/\left(10^{-pH} + 10^{-pK_a}\right)\right) \qquad (2)$$

In Fig. 7 a plot is shown of the effect of added [pyridine] on k_{obs} for methanolysis of 2.84×10^{-5} M fenitrothion promoted by 2×10^{-5} M **1** in the presence of 2 mM triethylamine buffer at ${}^{s}_{s}$pH 10.60 and 25 °C. The appearance of the plot is suggestive of the process exhibiting a common species rate depression given in Scheme 5 for which the kinetic expression given in eq. (3) is derived under the assumption of a steady state in [CH_3O^-:Pd(II):S=P]. The line through the data in Fig. 7 is derived from NLLSQ fitting of the data to eq. (3) where the calculated conditional constants at [**1**] = 2×10^{-5} M are $Kk_1 = 0.026$ M^{-1} s^{-1} and $k_{-1}/k_{cat} = 1.46 \times 10^5$ M^{-1}.

$$k_{obs} = K[\mathbf{1}]k_1/(1 + (k_{-1}/k_{cat})[Py]) \qquad (3)$$

From the above experiments, it was found that the reactivity difference for **3**, **1**, and **4** is 38:13:1. Since the concentration difference of the species **13** for the three palladacycles is not so high in the NMR experiments, this further indicates that species **13** can not be the major catalyst in our kinetic study.

2.5. Proposed mechanism of catalysis

Building upon what is proposed for related palladacycle-promoted hydrolyses of P=S pesticides [6,9], the kinetic data reported herein containing the common species rate depression in [pyridine] and the ordering of the k_2^{obs} data for **1**, **3** and **4** for the methanolysis of **5**, are consistent with the catalytic process given in Scheme 6 which requires two accessible *cis* sites on the palladacycle. One of these is required for substrate binding and the other for intramolecular delivery of a coordinated methoxide nucleophile to the transiently bound P=S unit. The results suggest that palladacycles **1**, **3** and **4**, when introduced into methanol solution, exist

Table 2
^{1}H NMR data for the speciation of palladacycles **1**, **3** and **4** (5×10^{-3} M) in methanol, for structures of the species see Scheme 4 in the text.

Palladacycle	Proton	Chemical shift of different species (ppm)			
		11	**12**	**13**	**14**
1	CH_2	4.07	4.04	3.83	
	$N(CH_3)$	2.81	2.77	2.71	
3	CH_2	4.10	4.09	3.83	
	$N(CH_3)$	2.83	2.80	2.71	
4	CH_2	4.00	3.98	3.83	
	$N(CH_3)$	2.77	2.76	2.71	
$Pd_2(dmba)_2Cl_2$	CH_2			3.86	3.94
	$N(CH_3)$			2.78	2.76

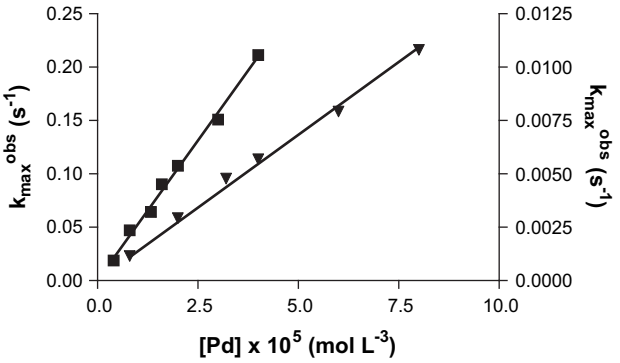

Fig. 5. Plots of k_{max}^{obs} vs. [Pd] of palladacycle **3** and **4** for the methanolysis of **5** [2.84×10^{-5} M] at 25 °C, TEA buffer (1–3) $\times 10^{-3}$ M, extrapolated to zero [buffer], ${}^{s}_{s}$pH 10.80. k_{max}^{obs} of **3** (■) corresponds to left *Y* axis, that of **4** (▼) corresponds to right *Y* axis.

Table 3
Second order rate constants (k_2^{obs}) from concentration dependence at the $^{s}_{s}$pH/log k_2 Kinetic data 10.80, and the maximum second order rate constants from fits to eq. (2) of the/log k_2 Kinetic data for the methanolysis of **5** catalyzed by palladacycles at [Pd] = 2.0×10^{-5} M, [**5**] = 2.84×10^{-5} M, 25 °C[a].

Palladacycles	k_2^{obs} (M^{-1} s^{-1})[a]	k_2^{max} (M^{-1} s^{-1})[b]	$^{s}_{s}pK_a$
1[c]	$(1.88 \pm 0.04) \times 10^3$	$(4.3 \pm 0.2) \times 10^3$	10.92 ± 0.04
3	$(5.24 \pm 0.09) \times 10^3$	$(15.1 \pm 0.9) \times 10^3$	11.04 ± 0.06
4	$(0.137 \pm 0.002) \times 10^3$	$(0.58 \pm 0.15) \times 10^3$	10.9 ± 0.2

[a] k_2^{obs} evaluated as the gradient of the k_{obs} vs [Pd] plots for each substrate under buffered conditions at 10.8.
[b] k_2^{max} and $^{s}_{s}pK_a$ computed on the basis of NLLSQ fits of the k_2^{obs} vs. $^{s}_{s}$pH data to the expression of eq. (2) derived for the process given in eq. (1).
[c] Data determined in this study; previously determined k_2^{max} and $^{s}_{s}pK_a$ values reported in ref. (5a) are 4.13×10^3 M^{-1} s^{-1} at $^{s}_{s}$pH 11.54 and 10.87.

predominantly as the mono-methanol complex, **11** in Scheme 4. The catalytically active forms are generated by ionization of **11** to form **12** having a kinetic $^{s}_{s}pK_a$ value between 10.8 and 11.0 for all three palladacycles, indicating the variations in pyridine substituents do not influence the ionization of the Pd-bound methanol to any great extent. The reactivity ordering (**3** > **1** > **4**) is consistent with an associative process where pre-equilibrium binding of the P═S unit with the Pd precedes the departure of the coordinated pyridine which is more facile for weak bases relative to strong ones. The required substitution of pyridine with the P═S containing substrate to form the kinetically competent species is suggested to arise from a typical bimolecular association [10,11] of the pesticide with the palladacycle to form a 5-coordinate associative complex or transient (not shown) from which expulsion of the pyridine occurs to give **15**. This is supported by the observed common species rate depression in added [pyridine] for the reaction of **1** with fenitrothion **5**. In addition, the observation that the kinetics for the methanolysis of **5** catalyzed by **1** [5a] as well as **3** and **4** depend linearly on the [palladacycle] indicates that no dimeric form such as **14** is important catalytically or as an inactive 'sink' for the Pd at these concentrations. The linearity also rules out a dissociative process where the pyridine ligand dissociates from the palladacycle prior to the capture of the P═S species since if the latter were operative, the concentration plot would exhibit downward curvature adhering to a square root dependence on [Pd]. Once formed, **15** reacts via intramolecular delivery of the *cis*-coordinated methoxide to the adjacent S═P unit with concomitant or subsequent expulsion of the aryloxy leaving group. The proposed Pd containing product of the later reaction is **16** which subsequently binds

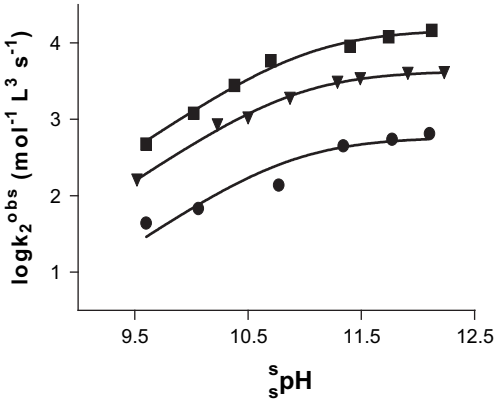

Fig. 6. Plots of log k_2^{obs} vs. $^{s}_{s}$pH for the methanolysis of **5** at [**5**] = 2.84×10^{-5} M, catalyzed by palladacycles **1**(▼), **3**(■), **4**(●), ([Pd] = 2.0×10^{-5} M) at 25 °C. Line through the data computed from fit to eq. (2); best fit k_2^{max} and kinetic $^{s}_{s}pK_a$ values listed in Table 4.

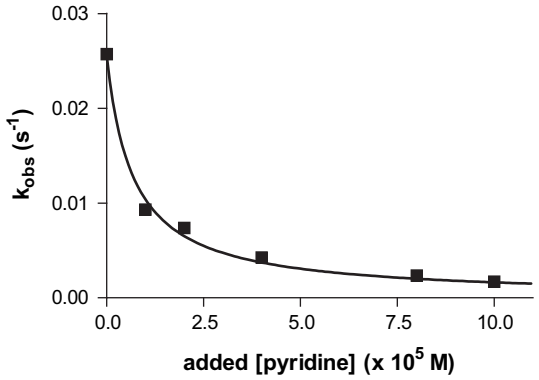

Fig. 7. Plot of the effect of added pyridine on the k_{obs} for methanolysis of 2.84×10^{-5} M fenitrothion promoted by 2×10^{-5} M **1** in the presence of 2 mM TEA buffer at $^{s}_{s}$pH 10.60, 25 °C. Data point at added [pyridine] = 0 taken from ref. (5a). Line through the data determined from NLLSQ fitting of the data to eq. (3) where $Kk_1 = 0.026$ s^{-1} and $k_{-1}/k_{cat} = 1.46 \times 10^5$ M^{-1}, $r^2 = 0.9941$, 6 data.

methoxide and pyridine with displacement of the $(RO)_2(CH_3O)P{=}S$ product to regenerate **12**.

In the case of the pincer compound **2**, the reaction is proposed to proceed analogously through the 5-coordinate associative species **18** either with expulsion of a (dimethylamino)methyl ligand to give a four coordinate species that reacts further, or without such dissociation by involving direct attack of the coordinated methoxide on the transiently bound P═S species. However, the slow rate of this process suggests that the reaction from putative **18** (Scheme 7) is not a particularly facile process, perhaps due to the greater distance of the coordinated methoxide from the P engendered by the large bite angle of 120° or more probably to the fact that dissociation of one of the benzyl amine ligands from the palladacycle to form a species analogous to **15** is far slower than dissociation of a pyridine.

According to the k_2^{max} values listed in Table 4, each of **1**, **3** and **4** is ~ 10^6 to 10^7 more active than free methoxide ion for promoting methanolysis of **5** (k_2 of methoxide is 7.2×10^{-4} M^{-1} s^{-1}) [5a]. Thus the computed half times for the methanolysis of **5** in the presence of 1 mM palladacycles **1**, **3** and **4** at $^{s}_{s}$pH 10.8 in methanol are 0.4, 0.13 and 5.1 s, respectively. Compared to the background methoxide promoted reaction at $^{s}_{s}$pH 10.80, the accelerations achieved by 1 mM of each of **1**, **3** and **4** are 2.1×10^9, 6.3×10^9, and 1.6×10^8, respectively.

2.6. Turnover experiments

The methanolysis of P═S pesticides fenitrothion (**5**), coumaphos (**6**), dichlofenthion (**7**), letophos (**8**), EPN (**9**), and phoxim (**10**) catalyzed by **3** under turnover conditions of excess substrate, was investigated by UV/vis spectroscopy under buffered conditions (1–2 mM TEA, $^{s}_{s}$pH 10.80, ambient temperature) in methanol. The observed first order rate constants (k_{obs}) and calculated k_2^{obs} values (computed as k_{obs}/[**3**]) are reported in Table 4. Complete methanolysis of these thiophosphates under turnover conditions has been confirmed by ^{1}H and ^{31}P NMR. However, at the higher concentration of P═S species used here relative to what was used in the kinetic studies, there is a 70-fold reduction in reactivity during the turnover experiment of fenitrothion **5** promoted by palladacycle **3**. This is attributable to the different concentrations of substrate (5-fold higher) and catalyst (4-fold lower) which could alter the solution and speciation properties. Nevertheless, these are still very effective catalytic systems for decomposition of these classes of pesticides, capable of forming non-toxic, methoxylated products under turnover conditions with good first order kinetics.

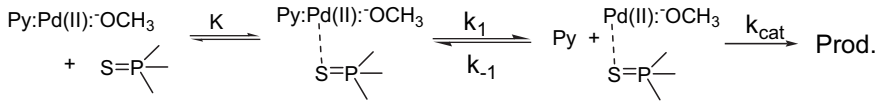

Scheme 5.

3. Conclusions

In the present study we have determined that the most effective catalysts for the methanolysis of thiophosphates are the *ortho*-palladacycles containing weakly coordinating pyridine with a strong electron-withdrawing group. The NCN'-pincer palladacycle (**2**) and *ortho*-palladacycles containing strongly binding monodentate ligands such as pyridines with strong electron donors are less active, considerably so in the case of **1** and **4**. The activity shown by the palladacycles **3** is among the highest demonstrated for the decomposition of phosphothionates, and is comparable or slightly higher than those reported for the hydrolysis of related substances. For example, Ryabov and coworkers reported k_2 values in the 200–900 M^{-1} s^{-1} range for the hydrolytic decomposition of parathion, methyl parathion $(CH_3O)_2P{=}S(OC_6H_4NO_2)$ and coumaphos promoted by a platinum complex and 57 M^{-1} s^{-1} for a palladacycle oxime at pH 8.5 in water [4d] while Gabbai and coworkers reported that methyl parathion is cleaved with a second order rate constant of 726 M^{-1} s^{-1} by a palladium oxazoline complex [6b] and $(8.6 \pm 3.6) \times 10^3$ M^{-1} s^{-1} at pH 9.0 by a [2-(2-pyridyl)phenyl-*C,N*]palladium complex [6c]. Of course in our cases the cleavage reactions are not hydrolytic ones, but methanolytic, meaning that the products are esters and not phosphorothioic acids which can introduce the possibility of inhibiting the catalysis of hydrolysis at higher pH through competitive binding of the palladacycle to the phosphorothionic acid products formed from the hydrolytic process. Further work on immobilizing these palladacycles on organic and inorganic polymers to make them recoverable and reusable are undertaken in our laboratory.

4. Experimental

4.1. Materials and methods

Methanol (99.8% anhydrous), sodium methoxide (0.5 M solution in methanol), silver triflate (AgOTf) and $HClO_4$ (70% aqueous solution) were commercial and used as-received. Fenitrothion (**5**, *O,O*-dimethyl *O*-(3-methyl-4-nitrophenyl) phosphorothioate), coumaphos (**6**, *O*-3-chloro-4-methyl-2-oxo-2H-chromen-7-yl *O,O*-diethyl phosphorothioate), dichlorofenthion (**7**, *O*-2,4-dichlorophenyl *O,O*-diethyl phosphorothioate), letophos (**8**, *O*-4-bromo-2,5-dichlorophenyl *O*-methyl phenylphosphonothioate), and EPN (**9**, *O*-ethyl *O*-4-nitrophenyl phenylphosphonothioate), and phoxim (**10**, *O,O*-diethyl *O*-(α-cyanobenzylideneamino) phosphorothionate) were purchased from Chem. Service Inc.

*Caution: all the phosphorus substrates described herein are acetylcholinesterase inhibitors; compounds **5**–**10** have oral LD_{50} values of 250, 16, 270, 43, 8, 300 mg kg^{-1}, respectively, in rats* [12].

^1H NMR and ^{31}P NMR spectra were recorded at 400 MHz and 161.97 MHz using a Brucker Avance-400 NMR spectrometer. ^1H NMR spectra were referenced to the $CD_2\mathbf{H}OD$ peak of d_4-methanol appearing at δ 3.31. ^{31}P-{^1H}-NMR spectra were referenced to an external standard of 70% phosphoric acid in water, and upfield chemical shifts are negative. Elemental analyses were performed on a GMBH Vario EL instrument. Mass-spectra were determined using a VG Quattro mass spectrophotometer equipped with an electrospray source. IR spectra were obtained in NaBr pellets using an AVATAR 360 FT-IR spectrometer. Melting points were measured on a Fisher-John melting point apparatus.

4.2. Preparation of palladacycles

General procedure: all organometallic syntheses were performed under a dried argon atmosphere.

4.3. 2,6-Bis(N,N-dimethylaminomethyl)phenyl(aqua)palladium(II) triflate, **2**

To a solution of 106 mg (0.32 mmol) of 2,6-bis(*N,N*-dimethylaminomethyl)phenylchloro-palladium(II) [13] in dichloromethane (20 mL) was added solid AgOTf (98.1 mg, 0.38 mmol, 1.2 eq.). The mixture was stirred at room temperature for 3 h and then filtered through celite. The celite was washed with another 20 mL of dichloromethane and the combined organics stripped of solvent by rotary evaporation under reduced pressure. The pale white solid residue was recrystallized from a mixture of hexanes and dichloromethane to afford 110.9 mg of crystals, yield 75%. m.p.: 195 °C. IR (KBr, cm^{-1}): 3388 br (νO–H), 2908 m (νC–H–alkyl), 1463 s (νC–H–arom.), 1259 vs (νC–N), 1169 vs, 1024 s (νS=O), 985 m, 946 m, 843 m, 760 m, and 639 m (δC–H–arom.), 515 m (νC–F). ^1H NMR (ppm, 400 MHz, d_4-methanol): δ 7.03 (t, $J = 8.0$ Hz, 1H), 6.84 (d, $J = 8.0$ Hz, 2H), 4.07 (s, 4H), 2.84 (s, 12H). ^{19}F NMR (ppm, 376.47 MHz, d_4-methanol): δ −81.1. MS (FAB): *m/z* 297.7 (M −OTf−H_2O). Anal. Calcd for $C_{13}H_{21}F_3N_2O_4PdS$ (Fw: 464.78) C 33.60, H 4.55, N 6.03%. Found: C 33.40, H 4.75, N 5.80%.

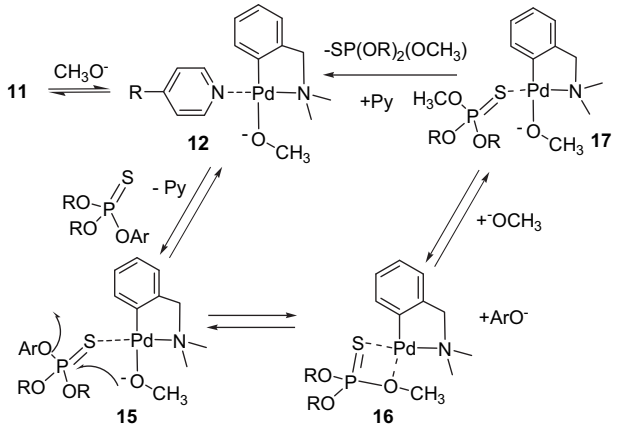

Scheme 6. Proposed mechanism for palladacycle-catalyzed methanolysis of P=S pesticides.

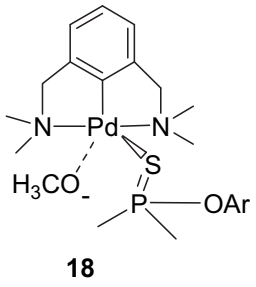

Scheme 7.

Table 4
Turnover conditional rate constants for the methanolysis of different phosphorothionate esters catalyzed by **3** (8.2×10^{-6} M) at 1 mM TEA, $^{s}_{s}$pH 10.80, 25 °C.

OP esters/(M)		TON	k^{obs} (s^{-1})	k_2^{obs} (M^{-1} s^{-1})	^{31}P NMR (ppm)	
					Substrate	Product
5	1.45×10^{-4}	17.7	8.6×10^{-4}	105	66.18	73.29
6	4.8×10^{-4}	58.5	2.1×10^{-3}	256	62.73	69.67
7	4.8×10^{-4}	58.5	9.8×10^{-3}	1195	63.29	69.60
8	1.6×10^{-4}	19.5	1.43×10^{-2}	1743	85.37	88.57
9	1.6×10^{-4}	19.5	1.52×10^{-2}	1854	88.85	90.92
10	1.6×10^{-4}	19.5	2.2×10^{-2}	268	68.4	69.0

Triflate complexes **3** and **4** were prepared from their corresponding chloride compounds which were synthesized from dichloro-bridged palladacycles containing the respective ligands and were obtained in good yield following the same procedure described for **1** [5a].

(*N*,*N*-Dimethylaminobenzyl-C^1,N)(4-trifuoromethylpyridine)(aqua)palladium(II) triflate, **3**: m.p.: 145 °C. IR (KBr, cm^{-1}): 3393 br ((νO–H), 1457 s, 1423 s (νC–H–arom), 1326 vs (νS=O), 1287 vs, 1256 vs (νC–N), 1175 s, 1142 s, 1032 s (νS=O), 840 m, 749 m, 638 m (δC–H–arom.), 518 m (νC–N). ^{1}H NMR (ppm, 400 MHz, d_4-methanol): 9.14 (d, J = 8.0 Hz, H$^{2'}$ and H$^{6'}$ on py), 7.93 (d, J = 8.0 Hz, H$^{3'}$ and H$^{5'}$ on py), 6.94 (m, H^3 and H^4 on phenyl), 6.66 (m, H^5 on phenyl), 5.81 (d, J = 8.0 Hz, H^6 on phenyl), 4.01 (s, CH_2), 2.73 (s, N(CH_3)$_2$–CH_2). ^{19}F NMR (ppm, 376.47 MHz, d_4-methanol): δ −67.73 (CF_3-py), −80.57 ($CF_3SO_3^-$). MS (FAB): m/z 387.70 (M − OTf–H_2O). Anal. Calcd for $C_{16}H_{18}F_6N_2O_4PdS$ (Fw: 554.78): C 34.64, H 3.27, N 5.05%; found: C 34.84, H 3.47, N 4.80%.

(*N*,*N*-Dimethylaminobenzyl-C^1,N)(4-*N*,*N*-dimethylaminopyridine)(aqua)palladium(II) triflate, **4**: m.p.: 155 °C. IR (KBr, cm^{-1}): 3364 br (νO–H), 2908 m (νC–H–alkyl), 1617 vs, 1534 s, and 1445 m (νC–H–arom.), 1385 m (νS=O), 1282 vs, 1254 vs, 1223 vs (νC–N), 1163 vs, 1030 vs (νS=O), 813 m, 743 m, and 639 m (δC–H–arom.), 520 m (νC–F). ^{1}H NMR (ppm, 400 MHz, d_4-methanol): 8.16 (d, J = 8.0 Hz, H$^{2'}$ and H$^{6'}$ on py), 6.89 (m, H^3 and H^4 on phenyl), 6.69 (d, J = 8.0 Hz, H$^{3'}$ and H$^{5'}$ on py), 6.63 (m, H^5 on phenyl), 5.97 (d, J = 8.0 Hz, H^6 on phenyl), 3.91 (s, CH_2), 3.03 (s, N(CH_3)$_2$ on py), 2.68 (s, N(CH_3)$_2$–CH_2). ^{19}F NMR (ppm, 376.47 MHz, d_4-methanol): δ −81.1 ($CF_3SO_3^-$). MS (FAB): m/z 362.77 (M − OTf − H_2O). Anal. Calcd for $C_{17}H_{24}F_3N_3O_4PdS$ (Fw: 529.85): C 38.54, H 4.57, N 7.93%; found: C 38.84, H 4.77, N 7.63%.

4.4. X-ray crystal structure determination

Crystals of **2**, **3**, and **4** suitable for diffraction measurements were prepared by slow diffusion of *n*-hexane into dichloromethane solutions of the corresponding palladacycles. A single crystal of each was mounted on a glass fiber with grease and cooled to −93 °C in a stream of nitrogen gas controlled with a Cryostream Controller 700. Data collection was performed on a Bruker SMART CCD 1000 X-ray diffractometer with graphite-monochromated Mo Kα radiation (λ = 0.71073 Å), operating at 50 kV and 30 mA over 2θ ranges of 3.72–50.00, 3.38–50.00, and 3.74–50.00 for **2**, **3**, and **4**, respectively. No significant decay was observed during the data collection.

Data were processed using the Bruker AXS Crystal Structure Analysis Package, Version 5.10 [14]. Neutral atom scattering factors were taken from Cromer and Waber [15]. The raw intensity data were integrated using the program SAINT-Plus. Absorption corrections were applied using the program SADABS [16].

In Table 5 the structural data for the data collection and refinement for palladacycle **2**, **3**, and **4** are given. In Table 1 selected bond lengths, bond angles and torsional angles for the three complexes are presented. ORTEP diagrams for each of **2**, **3**, and **4** at the 50% probability level are given in Figs. 1–3, respectively.

4.5. Kinetic methods

The $CH_3OH_2^+$ concentration was determined potentiometrically using a Radiometer GK2322 combination (glass/calomel) electrode

Table 5
Experimental data for the X-ray diffraction study on complexes **2**, **3**, and **4**.

Complex	**2**	**3**	**4**
Formula	$C_{13}H_{21}F_3N_2O_4PdS$	$C_{16}H_{18}F_6N_2O_4PdS$	$C_{17}H_{24}F3N_3O_4PdS$
Formula weight	464.78	554.78	529.85
T/K	180(2)	180(2)	180(2)
λ/Å	0.71073	0.71073	0.71073
Space group	P–1	P–1	P–1
a/Å	8.9818(6)	7.5282(5)	10.8703(10)
b/Å	9.1034(6)	11.2869(7)	11.4549(11)
c/Å	11.6323(8)	12.0748(7)	18.1335(18)
α/°	103.5930(10)	86.7580(10)	79.433(2)
β/°	101.4851(10)	86.2990(10)	89.316(2)
γ/°	97.8640(10)	84.0760(10)	75.941(2)
V/Å^3	888.97(10)	1017.10(11)	2151.94(4)
Z	2	2	4
ρ/g/cm^3	1.736	1.812	1.635
μ(mm^{-1})	1.210	1.094	1.012
F(000)	468	552	1072
Crystal size (mm)	0.35 × 0.30 × 0.25	0.40 × 0.30 × 0.20	0.30 × 0.20 × 0.10
θ/°	1.86 to 25.00	1.69 to 25.00	1.87 to 25.00
Index ranges	−10 <= h <= 10	−8 <= h <= 8	−12 <= h <= 12
	−10 <= k <= 10	−13 <= k <= 13	−12 <= k <= 13
	−13 <= l <= 13	−14 <= l <= 14	−20 <= l <= 21
Reflections collected	5153	5881	12686
Independent reflections	3108	3552	7551
	[R(int) = 0.0123]	[R(int) = 0.0157]	[R(int) = 0.0171]
Data/restraints/parameters	3108/0/229	3552/52/300	7551/0/546
Goodness-of-fit on F^2	1.060	1.070	0.920
Final R indices	R_1 = 0.0215,	R_1 = 0.0300,	R_1 = 0.0258,
[I > 2sigma(I)]	wR_2 = 0.0563	wR_2 = 0.0797	wR2 = 0.0509
Largest diff. peak and hole e Å^{-3}	0.408 and −0.512	1.044 and −0.679	0.431 and −0.336

calibrated with standard aqueous buffers (pH = 4.00 and 10.00) as-described in our recent paper [5a]. Values of $^{s}_{s}$pH [17] were calculated by subtracting a correction constant of −2.24 from the experimental meter reading as reported by Bosch et al. [18].

*4.5.1. Kinetics for methanolysis of **5***

The kinetics of methanolysis of fenitrothion (**5**) promoted by complexes **2**–**4** were monitored by observing the rate of appearance of 3-methyl-4-nitrophenol at 318 nm or 3-methyl-4-nitrophenolate at 404 nm using UV/visible spectrophotometry. All reactions were followed to at least three half-times at 25 ± 0.1 °C under buffered conditions. Buffers were prepared from *N*-methylmorpholine ($^{s}_{s}$pKa = 8.23), trimethylamine ($^{s}_{s}$pKa = 9.60), triethylamine ($^{s}_{s}$pKa = 10.78), and 2,2,6,6-tetramethylpiperidine ($^{s}_{s}$pKa = 11.86). The total [buffer] varied between 1 and 3×10^{-3} M and the buffers were partially neutralized with 70% $HClO_4$. To avoid any chloride ion contamination from the glass electrode that might affect the metal ion reactions duplicate solutions were prepared, one for the $^{s}_{s}$pH measurements, and the second for kinetic measurements. In all cases, $^{s}_{s}$pH values measured before and after reaction were consistent within 0.1 unit.

The first order rate constants (k_{obs}) determined under pseudo-first order conditions of a constant [catalyst] were evaluated by fitting the absorbance *vs.* time traces to a standard exponential model. The stock solutions of the palladium complexes **2**–**4** were prepared in pure methanol at 2×10^{-3} M. In order to determine the kinetic order in [palladacycle], a series of kinetic runs were undertaken at $^{s}_{s}$pH 10.80, (triethylamine buffer) using 2.84×10^{-5} M fenitrothion (**5**) in the presence of varying [palladacycle] from $(0.4–8) \times 10^{-5}$ M. The maximum pseudo-first order rate constants (k^{obs}_{max}) were obtained by extrapolating to [buffer] = 0.0 M (original data are given in Table S1 in supporting materials). The k_{obs} vs. [palladacycle] plots gave a straight lines (see Fig. 4), the gradients of which were taken as the second order catalytic rate constants (k^{obs}_{2}) listed in Table 3.

The $^{s}_{s}$pH dependences of the catalytic rate constants were determined by obtaining the k^{obs}_{max} rate constants for methanolysis of 2.84×10^{-5} M of **5** between $^{s}_{s}$pH 8.2 and 12.2 in the presence of a constant concentration of **3** and **4** (2.0×10^{-5} M) (data see Table S2 in supporting materials). The k^{obs}_{2} second order rate constants are obtained as $k^{obs}_{max}/(2 \times 10^{-5}$ M) and are plotted in Fig. 5.

4.5.2. Turnover experiments

To demonstrate that palladacycles were truly catalytic, turnover experiments of the methanolysis of an excess of substrates **5**–**10** (see Scheme 3) relative to palladacycle **3** were investigated in triethylamine buffer at $^{s}_{s}$pH 10.80 using UV/visible spectrophotometry and confirmed by ^{31}P NMR spectroscopy. The NMR data of the starting material and product signals are listed in Table 4.

In most cases, the intensity vs. time data adhered to good first order behavior for at least three half-times and standard fitting of the data to an exponential model yielded the first order rate constants given in Table 4 along with the turnover numbers. At higher concentration of substrates, the kinetic traces for some pesticides did not exhibit good first order kinetics so the rate constants in the table were computed only from the data where good first order behaviour was observed.

Acknowledgements

The authors gratefully acknowledge the financial assistance from Beijing Normal University (107026), Beijing Municipal Commission of Education, China, the Scientific Research Foundation for the Returned Overseas Chinese Scholars (213006), and Program for New Century Excellent Talents at Universities, The Ministry of Education, China.

Appendix A. Supplementary material

CCDC-710460 (for **2**), CCDC-710462 (for **3**), and CCDC-710461 (for **4**) contain the supplementary crystallographic data for this paper. These data can be obtained free of charge from The Cambridge Crystallographic Data Center via www.cccdc.cam.ac.uk/data-request/cif.

Supplementary data associated with this article can be found, in the online version, at doi:10.1016/j.jorganchem.2010.06.002.

References

[1] (a) A. Toy, E.N. Walsh, Phosphorus Chemistry in Everyday Living, second ed. American Chemical Society, Washington, DC., 1987, (Chapters 18–20);
(b) L.D. Quin, A Guide to Organophosphorus Chemistry. Wiley, New York, 2000;
(c) M.A. Gallo, N.J. Lawryk, Organic Phosphorus Pesticides. The Handbook of Pesticide Toxicology. Academic Press, San Diego, CA, 1991;
(d) P.J. Chernier, Survey of Industrial Chemistry, second ed. VCH, New York, 1992, pp. 389–417;
(e) K.A. Hassall, The Biochemistry and Uses of Pesticides, second ed. VSH, Weiheim, 1990, pp. 269–275.
[2] (a) Y.C. Yang, J.A. Baker, J.R. Ward, Chem. Rev. 92 (1992) 1729;
(b) Y.C. Yang, Acc. Chem. Res. 32 (1999) 109;
(c) Y.C. Yang, Chem. Ind. (London) (1995) 334;
(d) H. Morales-Rojas, R.S. Moss, Chem. Rev. 102 (2002) 2497 (and references therein).
[3] Conference on Disarmament, The Convention of the Development, Production, Stockpiling and Use of Chemical Weapons and on Their Destruction CD/1170. Geneva (August 1992) see. http://www.cwc.gov/cwc_treaty.html.
[4] (a) A. Chanda, S.K. Khetan, D. Banerjee, A. Ghosh, T.J. Collins, J. Am. Chem. Soc. 128 (2006) 12058;
(b) M.M. Higarashi, W.F. Jardim, Catal. Today 76 (2002) 201;
(c) L.Y. Kuo, N.M. Perera, Inorg. Chem. 39 (2000) 2103;
(d) G.M. Kazankov, V.S. Sergeeva, E.N. Efremenko, L. Alexandrova, S.D. Varfolomeev, A.D. Ryabov, Angew. Chem. Int. Ed. 39 (2000) 3117;
(e) J.C. Tao, J. Jia, X.W. Wang, S.T. Zang, Chin. Chem. Lett. 13 (2002) 1170;
(f) C.M. Hill, W.S. Li, J.B. Thoden, H.M. Holden, F.M. Raushel, J. Am. Chem. Soc. 125 (2003) 8990;
(g) B.M. Smith, Chem. Soc. Rev. 37 (2008) 470.
[5] (a) Z.L. Lu, A.A. Neverov, R.S. Brown, Org. Biomol. Chem. 3 (2005) 3379;
(b) B. Didier, M.F. Mohamed, E. Csaszar, K.G. Colizza, A.A. Neverov, R.S. Brown, Can. J. Chem. 86 (2008) 91;
(c) J.S.W. Tsang, A.A. Neverov, R.S. Brown, Org. Biomol. Chem. 2 (2004) 3457;
(e) S.A. Melnvchuk, A.A. Neverov, R.S. Brown, Angew. Chem. Int. Ed. 45 (2006) 1767;
(f) J.S. Tsang, A.A. Neverov, R.S. Brown, J. Am. Chem. Soc. 125 (2003) 7602;
(g) R.S. Brown, A.A. Neverov, J.S.W. Tsang, G.T.T. Gibson, P.J. Montoya-Pelaez, Can. J. Chem. 82 (2004) 1791;
(h) A.A. Neverov, R.S. Brown, Org. Biomol. Chem. 2 (2004) 2245;
(i) M.F. Mohamed, A.A. Neverov, R.S. Brown, Inorg. Chem. 48 (2009) 1183;
(j) T. Liu, A.A. Neverov, J.S.W. Tsang, R.S. Brown, Org. Biomol. Chem. 3 (2005) 1525.
[6] (a) M. Kim, F.P. Gabbaï, Dalton Trans. (2004) 3403;
(b) M. Kim, Q. Liu, F.P. Gabbaï, Organometallics 23 (2004) 5560;
(c) M. Kim, A. Picot, F.P. Gabbaï, Inorg. Chem. 45 (2006) 5600.
[7] J. Van den Broeke, J.J.H. Heeringa, A.V. Chuchuryukin, H. Kooijman, A.M. Mills, A.L. Spek, J.H. Van Lenthe, P.J.A. Ruttink, B.J. Deelman, G. Van Koten, Organometallics 23 (2004) 2287.
[8] A.D. Ryabov, G.M. Kazankov, A.K. Yatsimirskii, L.G. Kuz'mina, O.Y. Burtseva, N.V. Dvortsova, V.A. Polyakov, Inorg. Chem. 31 (1992) 3083.
[9] (a) A.D. Ryabov, G.M. Kazankov, S.A. Kurzeev, P.V. Samuleev, V.A. Polyakov, Inorg. Chim. Acta 280 (1998) 57;
(b) S.A. Kurzeev, G.M. Kazankov, A.D. Ryabov, Inorg. Chim. Acta 305 (2000) 1;
(c) G.M. Kazankov, V.S. Sergeeva, A.A. Borisenko, A.I. Zatsman, A.D. Ryabov, Russ. Chem. Bull. Int. Ed. 50 (2001) 1844.
[10] K.E. Frankcombe, K.J. Cavell, B.F. Yates, R.B. Knott, J. Phys. Chem. 100 (1996) 18363.
[11] (a) M. Schmuelling, A.D. Ryabov, R. van Eldik, J. Chem. Soc. Dalton Trans. (1994) 1257;
(b) M. Schmuelling, D.M. Grove, G. van Koten, R. van Eldik, N. Veldman, A.L. Spek, Organometallics 15 (1996) 1384.
[12] Pesticides and Metabolite Standard Catalogue. Chem. Services Inc., West Chester, Pennsylvania, 2006–2010.
[13] P. Steenwinkel, R.A. Gossage, T. Maunula, D.M. Grove, G. Van Koten, Chem. Eur. J. 4 (1998) 763.
[14] A.X.S. Brucker, Crystal Structure Analysis Package Version 5.10 (SMART NT (Version 5.053), SAINT-Plus (Version 6.01), SHELXTL (Version 5.1). Brucker AXS Inc., Madision, WI, USA, 1999.
[15] D.T. Cromer, J.T. Waber, International Tables for X-ray Crystallography. Kynoch Press, Birmingham, UK, 1974.

[16] G.M. Sheldick, Sadabs, 1996, Program for Area Detector Adsorption Correction. Institute of Inorganic Chemistry, University of Goettingen, Germany, 1996.
[17] For the designation of pH in non-aqueous solvents we use the forms recommended by the IUPAC, Compendium of Analytical Nomenclature. Definitive Rules 1997 3rd ed., Blackwell, Oxford, U.K. 1998. The term designates that 'pH' is measured in, and referenced to, the same solvent, which in the present case is methanol. Since the autoprotolysis constant of methanol is $10^{-16.77}$ neutral is 8.38.
[18] (a) E. Bosch, F. Rived, M. Roses, J. Sales, J. Chem. Soc. Perkin Trans. 2 (1999) 1953;
(b) I. Canals, J.A. Portal, E. Bosch, M. Roses, Anal. Chem. 72 (2000) 1802;
(c) F. Rived, M. Roses, E. Bosch, Anal. Chim. Acta 374 (1998) 309.